

## RESEARCH ARTICLE

## Analysis of the impact of IoT technology on marine salt spray particle detection and environmental protection equipment

Xianlian Mu<sup>1,2</sup>, Zebo Gu<sup>3,\*</sup>, Bin Li<sup>1</sup>, Xingxue Dai<sup>3</sup>, Chen Zhu<sup>3</sup>

<sup>1</sup>School of Aeronautics, Northwestern Polytechnical University, Xi'an, Shaanxi, China. <sup>2</sup>China Special Vehicle Research Institute, Key Laboratory of Corrosion Protection and Control of Aviation Technology, Jingmen, Hubei, China. <sup>3</sup>CVC Testing Technology Co., Ltd., Guangzhou, Guangdong, China.

Received: July 4, 2024; accepted: December 26, 2024.

In the marine environment, salt spray particles are defined as sea salt particles that are carried by tiny salt particles suspended in seawater. These particles are formed under the action of wind and constitute a component of marine meteorological phenomena, exerting a significant influence on marine ecology and human activities. In recent years, with the continuous promotion of the national marine strategy, the efficient operation and equipment safety of marine equipment have gradually received attention. In response to the problem of insufficient accuracy and real-time monitoring of salt spray particles in the marine environment, this study proposed a marine salt spray particle detection scheme based on Internet of Things technology and an improved YOLOv5l algorithm. By introducing spatial-to-depth convolution modules and convolutional block attention modules, the accuracy and robustness of the detection model had been significantly improved. The results showed that the model achieved excellent performance in terms of mean square error, root mean square error, and mean absolute error indicators as 0.000052, 0.0052, and 0.0011, respectively. The proposed model was superior to comparative algorithms of You Only Look Once-Gaussian Soft Selection and You Only Look Once-Convolutional Block Attention Module. The diagnostic accuracy of the proposed model was 92% with an interference capability of 36 dB, a sensitivity of 550 mV, and satisfactory real-time performance. The results indicated that the proposed model effectively improved the accuracy and real-time performance of marine salt spray particle detection, which was meaningful for improving the safe operation of marine equipment.

**Keywords:** internet of things technology; marine salt spray particle; environmental equipment; particle detection; YOLOv5l.

\*Corresponding author: Zebo Gu, CVC Testing Technology Co., Ltd., Guangzhou 510000, Guangdong, China. Email: [guzeb34@126.com](mailto:guzeb34@126.com).

### Introduction

Against the backdrop of China's strategic development in the South China Sea, the expansion of the country's maritime vision is accompanied by the widespread deployment of a series of domestically developed high-tech equipment in the region. However, the complex marine environment in the South China Sea poses a serious challenge to the safe and efficient

operation of this high-tech equipment due to its unique mechanical wear, chemical corrosion, and electrochemical effects [1, 2]. To address this challenge, the Internet of Things (IoT) technology, as an important means of real-time and accurate data collection, has shown great potential for application in marine environmental monitoring. The data collected through IoT technology can accurately calibrate and adjust device parameters, optimize operating modes,

and reduce energy consumption, which is crucial for ensuring the stable operation of devices in harsh environments [3, 4]. You Only Look Once version 5 large (YOLOv5l) is a real-time object detection algorithm based on deep learning, using larger models and deeper network structures to improve detection accuracy and robustness [5]. The YOLOv5l model employs a technique known as end-to-end training, whereby object detection tasks are transformed into regression problems, which enables the model to rapidly and accurately identify multiple objects within images or videos. Although IoT technology and related algorithms have shown significant advantages in marine environment monitoring, the complexity of existing research methods has become a major obstacle to their deployment on resource-limited edge devices. Consequently, many researchers are directing their attention to related research.

The advent of the IoT era has led more researchers to focus on applying IoT to various fields of life. Alassafi *et al.* proposed a method based on a Bidirectional Long Short-Term Memory (Bi-LSTM) network combined with optimization algorithms for the security detection of industrial IoT. This method had a detection accuracy of up to 98.91%, which was superior to existing methods, highlighting the importance of effective planning and innovative systems in improving industrial IoT network security [6]. Pragati *et al.* proposed a network security threat identification method based on a krill deep neural network stacked auto-encoder to address the vulnerability of IoT to network attacks. The accuracy of this method reached 99.37%, which was superior to 98% of the Support Vector Machine (SVM) and K-nearest Neighbor method (K-NN), as well as 90% and 92% of naive Bayes and random forests [7]. In addition, Asimkiran *et al.* applied genetic algorithms to select key features and trained a Convolutional Neural Network (CNN) model for network packet classification in the IDS method to address the vulnerability of the IoT environment of the MQTT protocol to attacks. This method could effectively identify potential

intrusions in MQTT networks with the satisfied test results [8]. Further, Geetha *et al.* proposed an intrusion detection method based on adaptive weighted kernel SVM and circular search to address the low fault detection rate of IoT systems in marine equipment environments. This approach had a detection rate of 93% on the UNSW-NB15 and KDD99 datasets, providing effective protection for marine equipment [9]. Ibrahim *et al.* proposed an image dimensionality reduction method combining edge computing and machine learning to solve the network traffic and delay problems caused by IoT device data transmission. After using auto-encoder and PCA dimensionality reduction, the data transmission volume was reduced by 77%, and there was no significant impact on the accuracy of cloud processing data [10]. Xu *et al.* proposed a method to introduce an attention mechanism in YOLO networks to address the issues of small object detection being susceptible to complex environmental background interference and poor detection results. This method improved the detection performance, and its effectiveness was further verified by creating amateur mask datasets and conducting experiments [11]. Further, Zhao *et al.* proposed the YOLO-AFPN model for detecting external damage targets in transmission lines, using techniques such as feature comparison, YOLOv8 network, and AFPN feature fusion to improve detection capabilities. The improved model had an average accuracy of 86.1% at a size of 6.6 MB, which was better than the original network and met the deployment requirements of edge devices [12]. Guo *et al.* designed a lightweight single-stage multi-object detection framework based on DCM3-YOLOv4 to address the challenges of accuracy and real-time performance in roadside sensing systems. The optimized model achieved a mAP of 0.930 and an inference time of 96.13 ms on the RS-UA dataset, outperforming other models on the same platform [13]. Previous studies have achieved significant results in improving IoT security and object detection. However, there are still some shortcomings. Although some developed methods have high detection accuracy, they sacrifice some real-time performance and may

not be suitable for application scenarios that require rapid response. In addition, some methods rely on numerous annotated data for training, requiring high quality and quantity of data. Some methods have high model complexity and are difficult to deploy on edge devices with limited resources. Therefore, there is an urgent need for a solution that can monitor Marine Salt Spray Particles (MSSP) in real-time with high accuracy and robustness. This solution requires no negative impact on real-time performance and does not impose excessive resource burden on edge devices.

In the marine environment, monitoring the atmospheric salt spray content is crucial for the safe operation of offshore equipment. The traditional monitoring method for marine salt spray is offline monitoring, which collects samples through gas collection methods such as the dry film method, analyzes sample data through spectrophotometry equipment and other methods after preprocessing, and obtains salt spray content through parameter conversion according to actual conditions [14, 15]. Such method can only monitor the salt spray content at a certain time point, and sampling requires a lot of manpower. IoT is a technology that connects entities in the real world to the Internet to realize the communication between things, people, and things, which can collect real-time information about objects that need to be monitored, connected, or interacted with through sensing devices. Moreover, IoT can be combined with DL algorithms. This study applied IoT technology to the monitoring of MSSP to achieve real-time monitoring of salt spray environments and then optimized the detection accuracy and robustness by improving the YOLOv5l algorithm (lYOLOv5l) and introducing Spatial-to-Depth Convolution (SPD-Conv) and Convolutional Block Attention Module (CBAM) to obtain an MSSP detection solution based on the IoT using lYOLOv5l, named lMSDPS-lY5l. The proposed Ocean Salt Spray Detection (OSSD) technology was expected to provide critical technical support for the efficient operation of marine equipment, significantly improve the

accuracy of MSSP detection, and provide strong guarantees for the safety and efficiency of offshore operations. This study also had the potential to promote the in-depth application of the IoT and deep learning technology in the marine environment, providing new research ideas and technological paths for the broad scientific and industrial sectors, which not only had important theoretical value but also had broad application prospects and a profound social impact.

## Materials and methods

### The proposed lMSDPS-lY5l environmental monitoring system

This study applied IoT technology to particle detection in Marine Salt Spray Environments (MSSE) and built an lMSDPS-lY5l system. The OSSD system was constituted of four layers including perception, network, application, and output (Figure 1). The main function of the perception layer was to collect parameters such as temperature, humidity, and pH value of the salt spray environment through sensing devices and used target detection and recognition technology to identify salt spray particles. The network layer was responsible for receiving data obtained by the perception layer. In the application layer, the data received in the network layer was transmitted to the cloud server through switches and routers [16]. The output layer interacted with humans through a web application to achieve real-time monitoring of salt mist particles at sea. In the design of the OSSD system perception layer, a salt spray environment could cause corrosion to the equipment, so it was necessary to add protective measures such as spraying anti-corrosion paint and galvanizing to the equipment. In the selection of sensors, it was necessary to ensure the accuracy of the sensors, and the sensors themselves needed to have storage functions, while also considering the economic efficiency of the sensors. Therefore, TH10S-B-PE temperature and humidity sensor (Shenzhen Inst Technology Co., Ltd., Shenzhen, Guangdong, China), the MIK-

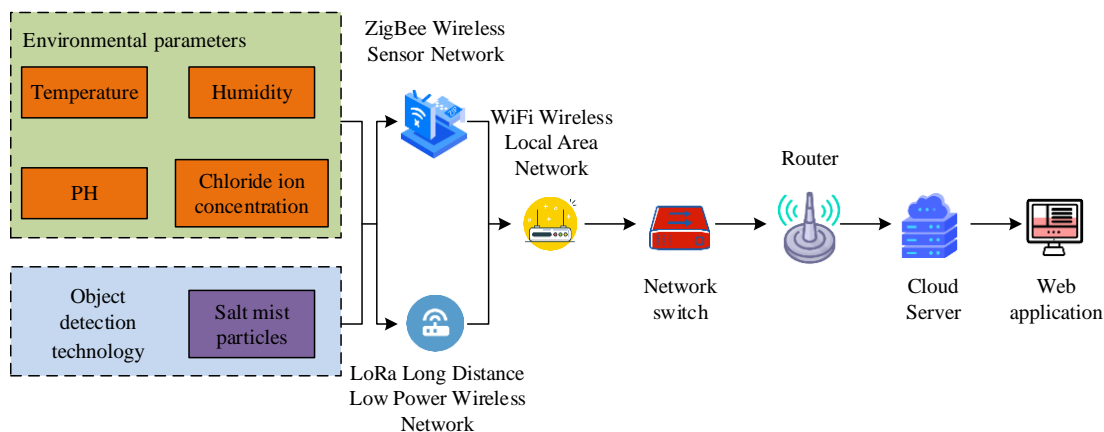


Figure 1. The architecture design of the IMSPDS-IY 51 system.

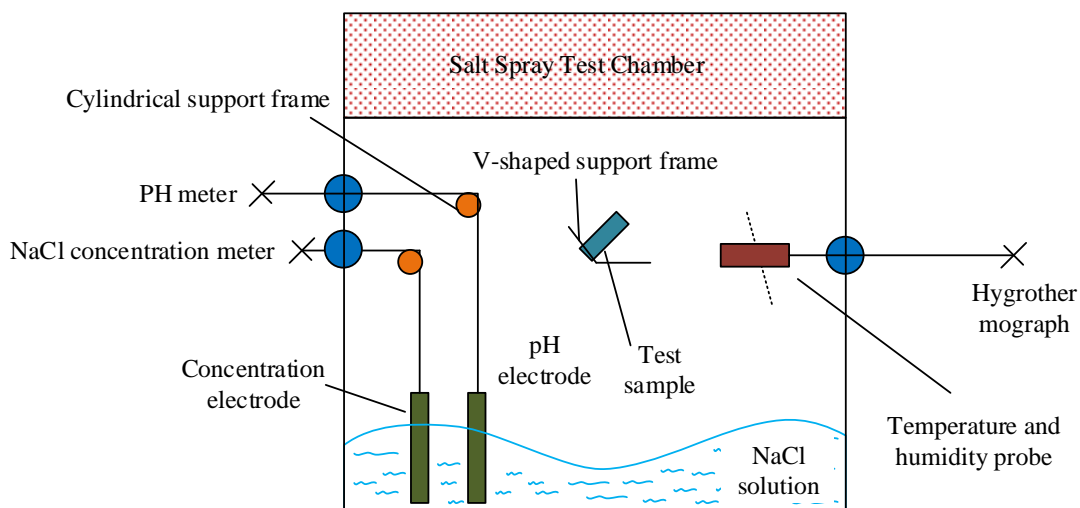


Figure 2. The layout and structure of the sensors.

PH2.0 pH meter (Hangzhou Mike Sensor Technology Co., Ltd., Hangzhou, Zhejiang, China), and the SJG-3083 sodium chloride concentration meter (Shanghai Boqu Instrument Co., Ltd., Shanghai, China) were selected in this research. All sensors used the Recommended Standard 485 (RS-485) interface and Modbus Remote Terminal Unit (RTU) as the network transmission protocol. The data collected by pH meters and sodium chloride concentration meters were the current environmental data. When detecting temperature and humidity, the closer the sensor was to the test sample, the closer the measured temperature and humidity were to the specific temperature and humidity of the current

environment. The layout of the sensors was shown in Figure 2. The monitored environmental indicators could better reflect the environmental conditions. For different scenarios, simply changing the parameters could obtain the corresponding environmental state. In the design of the network layer, it was essential to ensure that the data transmission line functioned correctly and reliably and that the data transmitted was of high integrity. At the same time, when building a network, the characteristics of the environment should be considered, and it was needed to ensure that the service life of the equipment was as high as possible. Due to the inconvenience of wiring at

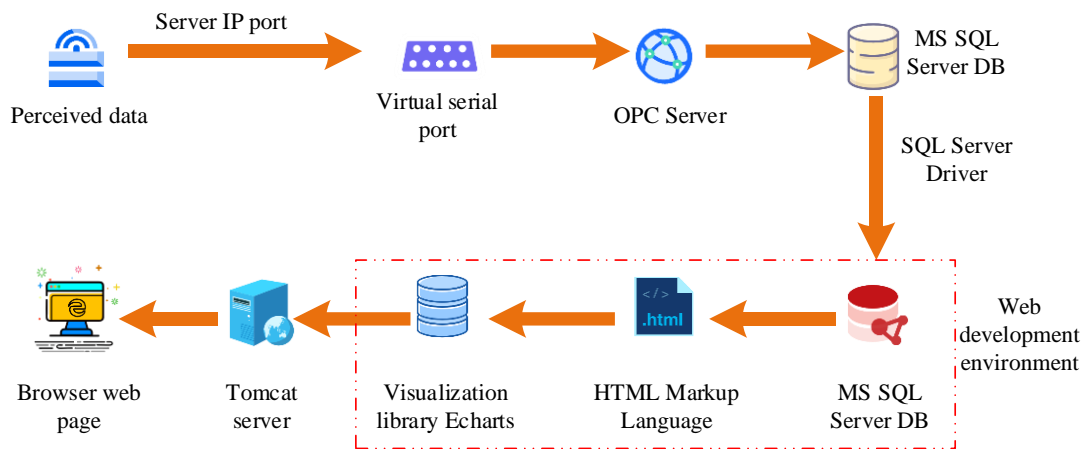


Figure 3. Data flow and processing process of the monitoring data.

sea, wireless communication should be chosen. There were many monitoring points and parameters for offshore facilities, and different compartments were separated, and there were also metal pipelines between compartments. Conventional wireless transmission networks could cause signal interruptions or transmission delays. When wireless signal transmission could not be achieved through the deployment of equipment compartments, heterogeneous networks could be used for layout. Therefore, this study constructed the network layer through multiple sensors, which included the ZigBee network used to obtain data from sensors in the perception layer, LoRa used as a wide area network to connect various sensor networks, a wireless local area network built through WIFI to connect the sensor network to the wide area network, data streams from multiple devices being exchanged and forwarded to the target devices through network switches to achieve communication between devices, and connecting to external servers through a router to achieve information sharing. The application layer was responsible for managing and monitoring data including data storage, output processing, and detecting web applications. The data flow and processing process of monitoring data were shown in Figure 3. After obtaining the data from the router, the detection data was saved in the MySQL server database using OPC server information system software through the

server IP port number and virtual serial port. The database was then connected to the web development environment through the MySQL server driver. In a web development environment, the detection data was first mapped using the Mybatis persistence layer framework, and then processed in the Springboot framework. The Hypertext Markup Language and ECharts data visualization icon library, asynchronous JavaScript, and XML web development technology were applied to achieve secondary development and web page refresh. After secondary development and debugging of all source files for detection data, it was necessary to check for errors. After confirming the accuracy, the detection data were packaged into a war compressed file through packaging operation and deployed to the Tomcat web server. The detection data was visualized using a web browser.

#### OSSD technology based on IYOLOv5l model

In MSSE monitoring, rapid and accurate detection of salt spray particle content is crucial for evaluating the corrosion resistance of offshore equipment in salt spray environments [17]. The corrosion resistance helps manufacturers understand the service life and performance of products in marine environments, providing a basis for product improvement and upgrading. Therefore, this study aimed to design a particle detection

algorithm suitable for MSSEs to accurately obtain salt spray content. YOLOv5l was used for the detection of salt spray particles, which was a variant of the YOLOv5 algorithm and adopted a larger model and deeper network structure based on YOLOv5, improving the model's robustness. The structure of YOLOv5l mainly contained a backbone network and multiple pyramid layers. The backbone was utilized to extract image features, while the feature pyramid layer could detect targets of different sizes at various scales. To further lift the performance of the YOLOv5l model, SPD-Conv was introduced in this study to capture fine-grained features. SPD-Conv is an innovative spatial encoding technique that can process images more effectively. In the SPD-Conv module, sub-features of output features could be obtained by slicing and calculated as follows.

$$f_{scale-1, scale-1} = X[scale-1: scale, scale-1: S: scale] \quad (1)$$

where  $scale$  was the scaling factor.  $X$  was the feature.  $f_{scale-1, scale-1}$  was the sub-features of the feature. After slicing, SPD-Conv concatenated all sub-features to obtain the output features of the input features in that layer. Meanwhile, in the cross stage of YOLOv5l, the Bottleneck Transformer module was added to the local connection module and combined into a new module. In this new module, three spatial convolutional layers were replaced with Multi-Head Attention (MHA) in the convolutional layer of the backbone network. By using self-attention to dynamically capture the intrinsic structure and semantic information of different input information, the correlation between various positional information could be obtained. In the Self-Attention Mechanism (SAM), after a vector was input into it, a function was learned to predict the output of any input vector as shown below.

$$f(x) = \sum_{i=1}^n \frac{K(x-x_i)}{\sum_{j=1}^n K(x-x_j)} y_i \quad (2)$$

where  $f(x)$  was the learned function.  $i$  and  $j$  were the  $i$ -th and  $j$ -th input vectors.  $n$  and  $y_i$  were the total number and output of input vectors.  $K$  was the weight. When calculating the output of self-attention, the embedding operation was first performed to transform the input vector into an intermediate vector. Then, the intermediate vector was multiplied by the weight matrix to obtain the query, value, and the key that matched each value as shown below.

$$\begin{cases} q^i = W^q a^i \\ k^i = W^k a^i \\ v^i = W^v a^i \end{cases} \quad (3)$$

where  $a^i$  was the intermediate vector.  $q^i$  was the query.  $v^i$  was the value.  $k^i$  was the key.  $W^q$ ,  $W^k$ , and  $W^v$  were the weight matrices of the query, key, and value, respectively. Among them, the query was used to match with other words, *i.e.* the query target. The key was used to match the query. Queries, keys, and values could be transformed into matrix form as shown in equation (4).

$$\begin{cases} Q = W^q I \\ K = W^k I \\ V = W^v I \end{cases} \quad (4)$$

where  $I$  was the matrix composed of intermediate vectors. The output of the SAM was shown in equation (5).

$$Attention(Q, K, V) = softmax\left(\frac{QK^T}{\sqrt{d_k}}\right)V \quad (5)$$

where  $Attention(Q, K, V)$  was the output of the SAM.  $d_k$  was the dimension of the query.  $softmax$  was the activation function. By combining multiple single SAMs to form an MHA mechanism, integrating the outputs of all single SAM through concatenation operations, and then mapping the concatenated results through a weight matrix, the output of MHA could be

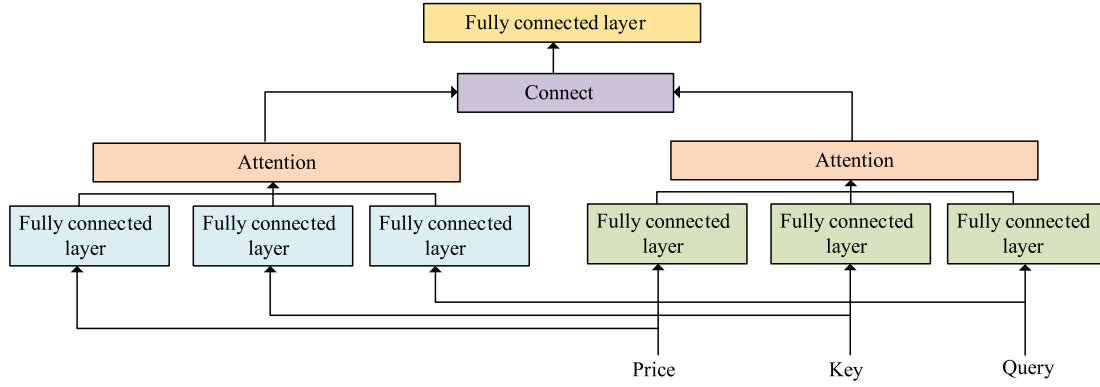


Figure 4. Schematic diagram of MHA mechanism structure.

calculated as follows.

$$MultiHead(Q, K, V) = Concat(head_1, \dots, head_h)W_0 \quad (6)$$

where  $MultiHead(Q, K, V)$  was the output of MHA.  $head_h$  was the  $h$ -th self attention.  $W_0$  was the weight matrix for adjusting the output dimension. SAM and MHA mechanism structures were shown in Figure 4. To improve the feature extraction capability of YOLOv5l network, this study introduced CBAM in the downsampling module of the network. The features were input into the regular convolution block to obtain the intrinsic features of the input features as shown in equation (7).

$$Y_c = Mish(B(f^{3 \times 3}(X) + b)) \quad (7)$$

where  $Y_c$  was the intrinsic feature of the input data.  $f^{3 \times 3}$  was  $3 \times 3$  convolution operation.  $B$  was the batch normalization layer.  $Mish$  was the activation function.  $b$  was the bias.  $c$  was the number of channels. The residual blocks were then added after the convolution module to further obtain features as shown in equation (8).

$$\begin{cases} Y' = Mish(B(f^{1 \times 1}(Y_c))) \\ Y'' = Mish(B(f^{1 \times 1}(Y')) + Y_c) \end{cases} \quad (8)$$

where  $Y''$  was the feature after residual processing. Then, using deep convolution, the output feature map was linearly computed to

obtain feature information as shown in equation (9).

$$Y_{cv} = \varphi_{cv}(Y''), \forall c \in [1, m], v \in [1, s] \quad (9)$$

where  $Y_{cv}$  was the feature obtained from the  $v$ -th linear calculation of the feature on the  $c$ -th channel.  $\varphi_{cv}$  was a linear computational function. The acquired features were then compressed in the CBAM module. The multi-layer perceptron was used to output the processed feature vectors. The feature vectors were summed and calculated through activation functions to obtain channel attention as shown in equation (10).

$$\begin{cases} M_c(X) = \sigma(W_1(W_2(F_{avg}^c)) + W_1(W_2(F_{max}^c))) \\ F' = M_c(X) \otimes X \end{cases} \quad (10)$$

where  $W_1$  and  $W_2$  were the weight matrices of two fully connected layers in a multi-layer perceptron, respectively.  $F_{avg}^c$  was the output of the average pooling layer.  $F_{max}^c$  was the output of the maximum pooling layer.  $\sigma$  was the sigmoid activation function.  $\otimes$  was element wise multiplication.  $F'$  was the feature map. A convolution of  $7 \times 7$  was used to further process the features and obtain a spatial attention feature map with the calculation below.

$$M(F') = \sigma(f^{7 \times 7}([F_{avg}^s; F_{max}^s])) \quad (11)$$

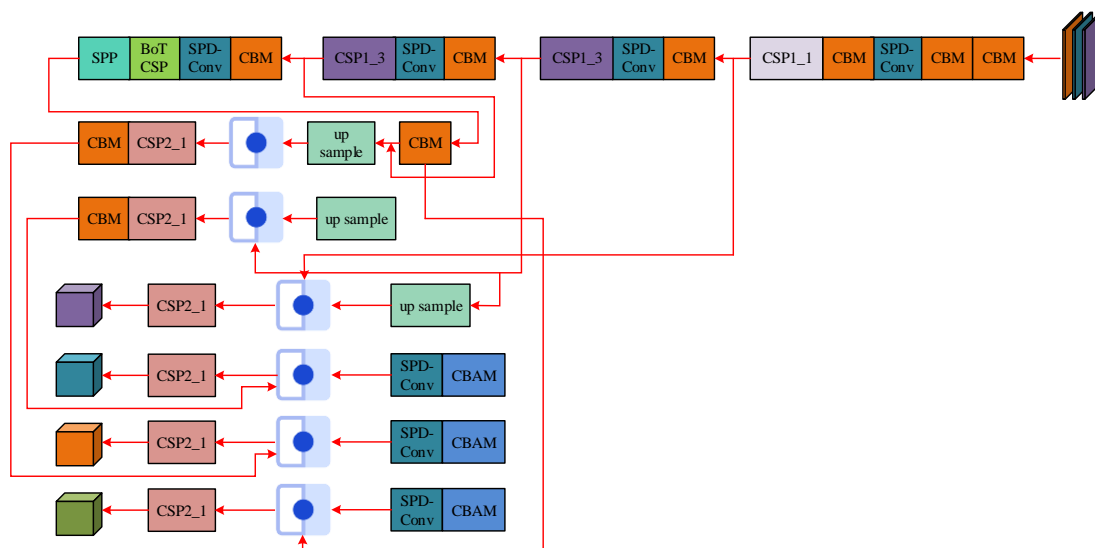


Figure 5. Schematic diagram of the YOLOv5l technical flow.

where  $F'$  was the spatial attention feature map.  $f^{3 \times 3}$  was the  $7 \times 7$  convolution operation. The output features could be obtained by multiplying the feature map and spatial feature map element by element as shown in equation (12).

$$F = M(F') \otimes F' \quad (12)$$

where  $F$  was the final output result. The designed IYOLOv5l process was shown in Figure 5. To verify the superiority of the performance of the proposed IYOLOv5l model, experiments were conducted using Focal Loss for Dense Object Detection (RetinaNet) (<https://github.com/MegEngine/Models>), Region-based CNN for Instance Segmentation (Mask R-CNN) ([https://github.com/matterport/Mask\\_RCNN](https://github.com/matterport/Mask_RCNN)), Region-based Full Convolutional Network (R-FCN) (<https://github.com/daijifeng001/R-FCN>), and Scalable and Efficient Object Detection (EfficientDet) (<https://github.com/zylo117/Yet-Another-EfficientDet-Pytorch>) algorithms for horizontal comparison. The above algorithms were implemented using Python 3.8 (<https://www.python.org>) on Windows 10 operating system equipped with Intel Core i9-13900H CPU, GeForce RTX 3080 Ti graphics processor, 32 GB of running memory, and 12 GB

of graphics card memory. The maximum iteration for the IYOLOv5l was set to 300, the batch size was 8, the weight decay coefficient was 0.0005, and the initial learning rate was 0.01. To further verify that the proposed IMSPDS-IY5l technology also performed similarly well in practical applications, the improved YOLOv8 fault detection scheme [18], You Only Look Once-Gaussian Soft Selection (YOLO-GSS) [19], and YOLO\_CBAM [20] were employed to compare with IMSPDS-IY5l. Diagnostic accuracy, anti-interference ability, sensitivity, real-time performance, and diagnostic speed were taken as the evaluation indicators. To verify the effectiveness of the IYOLOv5l algorithm, this study compared to YOLOv5l with the same 6,000 data samples from marine salt spray particle database (MSSPD), which included information on the concentration, size distribution, shape characteristics, and chemical composition of salt spray particles. Data were collected from offshore experimental platforms, laboratory simulated salt spray environments, historical monitoring data, etc. and covered a period of 3-5 years.

## Results and discussion



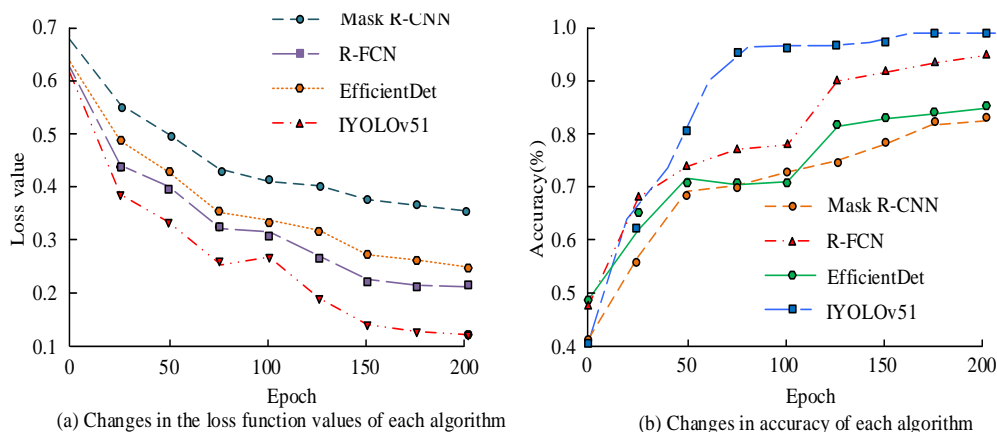


Figure 6. Comparison of loss function value (a) and accuracy (b) of different algorithms.

### Performance of IYOLOv5l model

Compared with other detection algorithms, the IYOLOv5l completed lower values in the three evaluation indicators of Mean Square Error (MSE), Root Mean Square Error (RMSE), and Mean Absolute Error (MAE). The MSE of IYOLOv5l was 0.000052, which was significantly lower than RetinaNet's 0.000125, Mask R-CNN's 0.000131, R-FCN's 0.000091, and EfficientDet's 0.000073. Similarly, on RMSE and MAE, IYOLOv5l also demonstrated significant superiority, indicating that the predicted values during training were closer to the true values (Table 1). The results verified that the IYOLOv5l model was indeed superior in performance to other popular object detection algorithms.

Table 1. Performance comparison of different models.

Model	MSE	RMSE	MAE
RetinaNet	0.000125	0.0132	0.0023
Mask R-CNN	0.000131	0.0123	0.0064
R-FCN	0.000091	0.0081	0.0054
EfficientDet	0.000073	0.0083	0.0043
IYOLOv5l	0.000052	0.0052	0.0011

### The accuracy and loss value of the proposed model

Four algorithms of Mask R-CNN, R-FCN, EfficientDet, and IYOLOv5l were compared for the performance accuracy and loss value. The

results showed that the proposed IYOLOv5l performed well during the training process with its loss value rapidly decreasing from the beginning of training and eventually stabilizing at a low level of 0.05 (Figure 6a). In contrast, the loss function values of Mask R-CNN, R-FCN, and EfficientDet tended to approach 0.38, 0.23, and 0.31, respectively, significantly higher than that of IYOLOv5l. The results demonstrated that the accuracy of IYOLOv5l rapidly improved from the early training stage and eventually converged to 0.96, while the loss function values of Mask R-CNN, R-FCN, and EfficientDet algorithms converged to 0.38, 0.23, and 0.31, respectively (Figure 6b).

### Comparison of YOLOv5l algorithm before and after improvement

The results showed that the accuracy of the YOLOv5l algorithm before improvement was around 75% on average when the sample size was 1,000. As the samples increased, its accuracy also steadily improved. When the samples reached 5,000, the accuracy of the algorithm stabilized at around 85% (Figure 7a). The improved IYOLOv5l algorithm had a high accuracy level when the sample size was 1,000. When the sample size reached 5,000, its accuracy stabilized at around 96% (Figure 7b). These results indicated that the IYOLOv5l algorithm had shown significant advantages in accuracy, performance stability, and learning efficiency, therefore the improved method was successful.

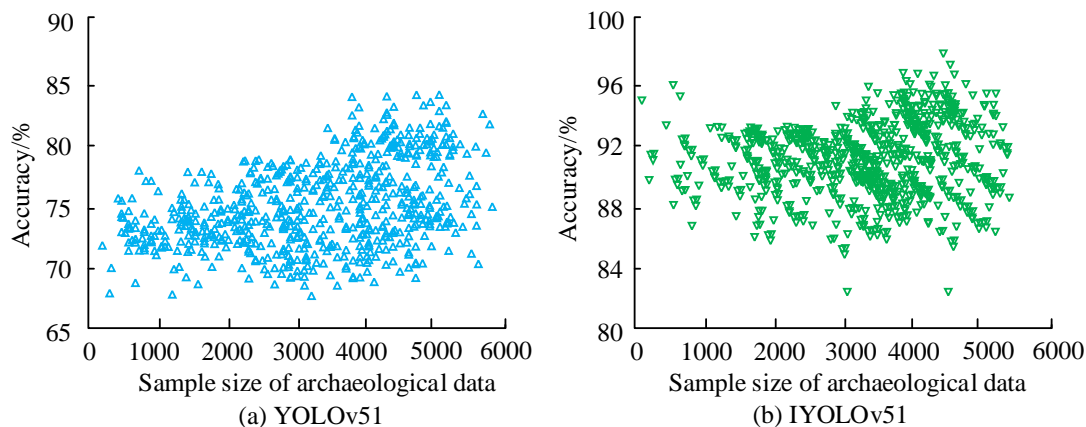


Figure 7. The accuracy changes of YOLOv5l before (a) and after (b) the improvement.

Table 2. Comparison of the practical application effects of different test schemes.

Schemes	Diagnostic accuracy (%)	Anti-interference capability (dB)	Sensitivity (mV)	Real-time performance (ms/frame)	Diagnostic speed (frame/s)
Improved YOLOv8	85	28	450	120	15
YOLO-GSS	88	30	480	100	20
YOLO_CBAM	90	34	520	95	25
MSPDS-IY5l	92	36	550	80	30

### Application results of IMSPDS-IY5l scheme

The results of 100 repeated experiments on detecting MSSP in actual environments demonstrated that the MSPDS-IY5l scheme showed superiority in all evaluation indicators with its diagnostic accuracy as high as 92%, which was significantly higher than the other three schemes, indicating that this proposed scheme had a stronger recognition ability for MSSP in practical applications (Table 2). Meanwhile, the anti-interference ability of MSPDS-IY5l was also the strongest one, reaching 36 dB, which meant that the scheme could work more stably in the face of complex environmental interference. In addition, MSPDS-IY5l had the highest sensitivity at 550 mV, indicating a more sensitive detection of MSSP. In terms of real-time performance, MSPDS-IY5l only took 80 ms to process each frame of the image with the diagnostic speed reaching 30 frames per second, which was the best among all compared schemes, ensuring faster response and diagnosis in practical applications. Through IoT technology, real-time and accurate data could be collected from the

marine environment including salinity, temperature, humidity, etc. These data could help environmental equipment calibrate and adjust its operating parameters more accurately, optimize the operating mode and energy consumption of the equipment, and improve energy utilization efficiency. This study utilized improved YOLOv8, YOLO-GSS, YOLO\_CBAM, and MSPDS-IY5l technology for 96 Marine Communication Base Stations (MCBSs). The energy utilization efficiency of each base station was used as the evaluation index. The results showed that the average energy utilization rates (AEURs) of 24 MCBS in each Improved YOLOv8, YOLO-GSS, YOLO\_CBAM, and MSPDS-IY5l technologies were 43.3%, 45.6%, 38.4%, and 71.2%, respectively (Figure 8). IoT technology could monitor the operational status of devices in real-time and detect abnormal situations promptly. To explore the impact of MSPDS-IY5l technology on environmental equipment, this study conducted comparative experiments. The efficiency and accuracy of environmental equipment were evaluation indicators. The

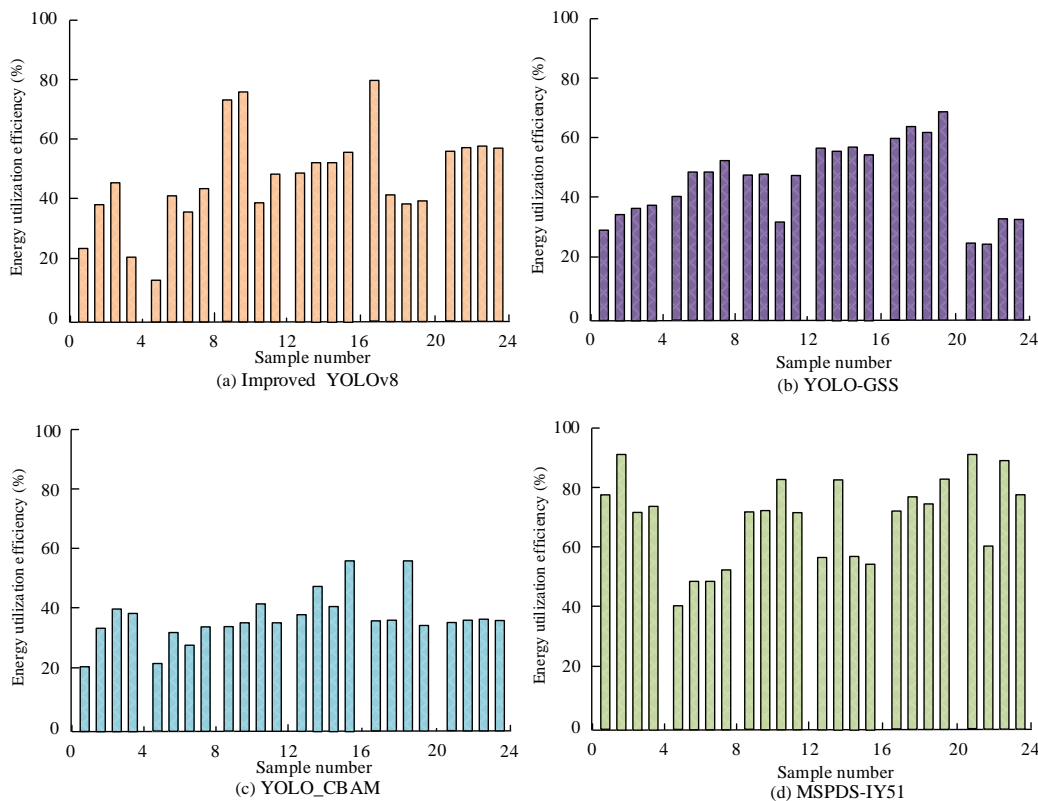


Figure 8. The average energy utilization rates of each scheme on the energy efficiency of MCBSs.

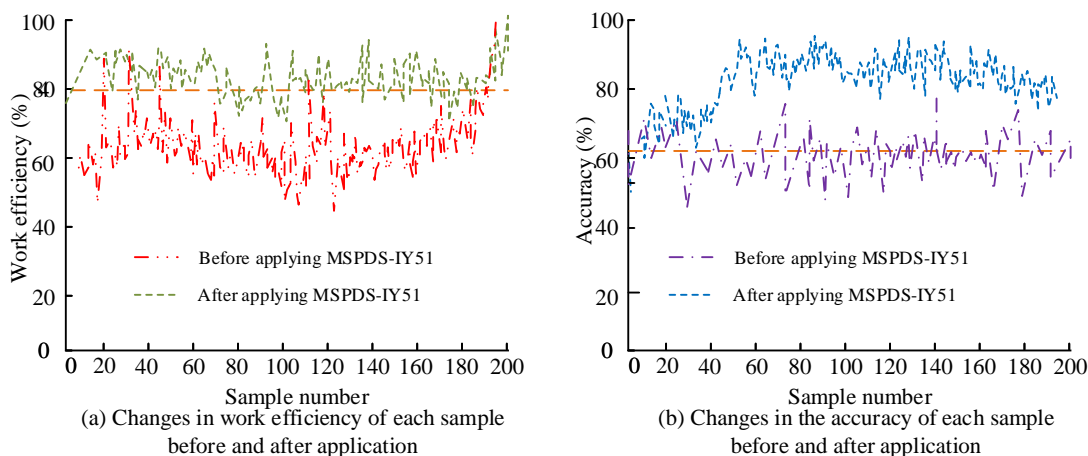


Figure 9. Changes in working efficiency (a) and accuracy (b) of each sample before and after the application of MSPDS-IY51 technology.

results demonstrated that MSPDS-IY51 technology had a significant positive impact on environmental equipment. Through comparative analysis, the application of this technology had significantly improved the work efficiency and accuracy of the samples. The work efficiency had

increased from 70% to over 80%, which meant that more work tasks could be completed within the same time, thereby improving the overall operational efficiency of environmental equipment (Figure 9). The work accuracy had also significantly improved, jumping from 60% to over

85%, indicating that MSPDS-IY5I could significantly reduce work errors and enhance the stability and reliability of environmental equipment. MSPDS-IY5I had an obvious effect on improving the efficiency and accuracy of environmental equipment, demonstrating the practical application value of this technology.

### Conclusion

This study proposed an IMSPDS-IY5I detection scheme to address the challenges faced by equipment in MSSEs. By introducing SPD-Conv and CBAM, the accuracy and robustness of the detection model had been greatly improved. The results showed that the IYOLOv5I model achieved significant advantages in MSE, RMSE, and MAE indicators, reaching 0.000052, 0.0052, and 0.0011, respectively. In practical applications, the IMSPDS-IY5I scheme outperformed other comparative schemes in diagnostic accuracy, anti-interference ability, sensitivity, *etc.*, especially in terms of energy utilization efficiency, achieving an AEUR of 71.2%. Meanwhile, work accuracy had been significantly improved, jumping from 60% to over 85%, indicating that MSPDS-IY51 technology could significantly reduce work errors. MSPDS-IY51 only took 80 ms to process each frame of the image, and the diagnostic speed reached 30 fps, which was the best among all schemes, ensuring faster response and diagnosis in practical applications. This study provided an effective means for equipment monitoring in MSSEs and new ideas for the application of IoT in the field of environmental monitoring. Although significant achievements had been made in marine OSSD research, the detection performance of the model under extreme environmental and weather conditions still needed further validation and optimization.

### Acknowledgements

The research was supported by Research on numerical simulation techniques for

condensation behavior of electronic devices in marine environments (Grant No. 2023000205001).

### References

1. Choudhuri S, Adeniye S, Sen A. 2023. Distribution alignment using complement entropy objective and adaptive consensus-based label refinement for partial domain adaptation. *Artificial Intelligence and Applications*. 1(1):43-51.
2. Long XM, Chen YJ, Zhou J. 2023. Development of an AR experiment on electric-thermal effect by open framework with simulation-based asset and user-defined input. *Artificial Intelligence and Applications*. 1(1):52-57.
3. Islam A, Othman F, Sakib N, Babu HMH. 2023. Prevention of shoulder-surfing attack using shifting condition with the digraph substitution rules. *Artificial Intelligence and Applications*. 1(1):58-68.
4. Wu XQ, Qian SR, Yang M. 2023. Detection of safety helmet-wearing based on the YOLO\_CA model. *Comput Mater Contin*. 77(3):3349-3366.
5. Ji C, Zhang F, Huang X, Song Z, Hou W, Wang B, *et al.* 2023. STAE-YOLO: Intelligent detection algorithm for risk management of construction machinery intrusion on transmission lines based on visual perception. *IET Gener Transm Distrib*. 18(3):542-567.
6. Alassafi MO, Hasan SH, Badri S, Hasan SH. 2024. Optimized Bi-LSTM: A novel approach for attack detection in industrial IoT. *Signal Image Video Process*. 18(5):4903-4913.
7. Rana P, Chauhan S, Patil BP. 2024. Cyber security threats detection in IoT using krill based deep neural network stacked auto encoders. *Wirel Pers Commun*. 135(1):299-322.
8. Asimkiran D, Bhaskar M. 2024. Design of intrusion detection system using GA and CNN for MQTT-based IoT networks. *Wirel Pers Commun*. 134(4):2059-2082.
9. Geetha C, Johnson SD, Oliver AS, Lekha D. 2024. Adaptive weighted kernel support vector machine-based circle search approach for intrusion detection in IoT environments. *Signal Image Video Process*. 18(5):4479-4490.
10. Ibrahim A, Khaled W, Hanaa B. 2024. Dimensionality reduction for images of IoT using machine learning. *Sci Rep*. 14(1):7205.
11. Xu C, Dong Z, Zhong S, Chen Y, Pan S, Wu M. 2024. Fusion network for small target detection based on YOLO and attention mechanism. *Optoelectron Lett*. 20(6):372-378.
12. Zhao Z, Pan Y, Guo G. 2024. YOLO-AFPN: Marrying YOLO and AFPN for external damage detection of transmission lines. *IET Gener Transm Distrib*. 18(9):1935-1946.
13. Guo BC, Wang HH, Han ZT, Zhang SR. 2024. DCM3-YOLOv4: A real-time multi-object detection framework. *Automotive Innov*. 7(2):283-299.
14. Ding Z, Ning J, Zhou Y, Kong A, Duo B. 2024. Detecting landslides with deformable adaptive focal YOLO: Enhanced performance with reduced false detection. *PFG-J Photogramm Rem*. 92(2):115-130.
15. Mukesh C, Sonu R, Vimal K. 2024. Deep learning-based framework for the observation of real-time melt pool and

- detection of anomaly in wire-arc additive manufacturing. *Mater Manuf Process.* 39(6):761-777.
16. Anilkumar C, Rani MS, Venkatesh B, Rao GS. 2024. Automated license plate recognition for non-helmeted motor riders using YOLO and OCR. *J Mob Multimedia.* 20(2):239-266.
  17. Sugashini T, Balakrishnan G. 2023. YOLO glass: Video-based smart object detection using squeeze and attention YOLO network. *Signal Image Video Process.* 18(3):2105-2115.
  18. Chen F, Deng M, Gao H, Yang X, Zhang D. 2024. NHD-YOLO: Improved YOLOv8 using optimized neck and head for product surface defect detection with data augmentation. *IET Image Process.* 18(7):1915-1926.
  19. Hou C, Li Z, Shen X, Li G. 2024. Real-time defect detection method based on YOLO-GSS at the edge end of a transmission line. *IET Image Process.* 18(5):1315-1327.
  20. Li J, Zhao M, Qin Z, Yuan R, Huang A, Li M. 2024. Detection and recognition of multiple QR codes based on YOLO\_CBAM algorithm. *Int J Bio-Inspir Com.* 23(3):179-188.